Aura Microwave Limb Sounder Observations of the Northern Annular Mode: From the Mesosphere to the Upper Troposphere

Jae N. Lee[1], Dong L. Wu[2], Gloria L. Manney[2,3], and Michael J. Schwartz[2]

1. NASA Postdoctoral Program Fellow, Jet Propulsion Laboratory, California Institute of Technology, Pasadena, CA
2. Jet Propulsion Laboratory, California Institute of Technology, Pasadena, CA
3. New Mexico Institute of Mining and Technology, Socorro, NM

Abstract

Vertical structure and evolution of the wintertime Northern Hemisphere Annular Mode (NAM), the first Empirical Orthogonal Function (EOF) of geopotential height anomalies, are constructed from the 2005-2009 Aura Microwave Limb Sounder (MLS) measurements in the entire middle atmosphere between 316 hPa (~9 km) and 0.001 hPa (~90 km). This is the first report of NAM structure extending into the mesosphere. The mode appears to be robust and it accounts for up to 70% of middle-atmospheric variance before dropping off in the upper mesosphere. The vertical connection of the NAM modes suggests strong dynamic coupling between the mesosphere and stratosphere. Time evolution of the NAM suggests that the significant NAM anomalies typically appear first in the mesosphere and progress downward. NAM patterns derived from MLS observations are consistent with those derived from long-term reanalysis below the middle stratosphere. Mesospheric cooling signals precede the major SSW signals by up to 4 weeks.

1. Introduction

The Northern Hemisphere annular mode (NAM), an approximately axially symmetric perturbation of arctic geopotential height (GPH) relative to that of mid-latitudes, is the leading empirical orthogonal function (EOF) of GPH in the northern winter from the upper mesosphere down to at least the upper troposphere. The time-varying strength of this mode is an important tool for diagnosing variability of the winter polar atmosphere [*Thompson and Wallace*, 1998; 2000]. The vertical coherence of the winter NAM pattern plays a fundamental role in the stratosphere-troposphere coupling, both in observations [e.g., *Baldwin and Dunkerton*, 1999; 2001; *Black*, 2002] and in model simulations [e.g., *Limpasuvan and Hartmann*, 2000; *Plumb and Semeniuk*, 2003; *Kushner and Polvani*, 2004; *Hardiman and Haynes*, 2008]. Effects of solar variability on the atmosphere are also apparent in the NAM [*Baldwin and Dunkerton*, 2004; *Hameed and Lee*, 2005; *Lee and Hameed*, 2007].

Polar stratosphere-to-troposphere coupling events are often preceded by a disturbance in the upper atmosphere. *Baldwin and Dunkerton* [1999] found that large anomalies of the Northern Hemisphere (NH) wintertime stratospheric polar vortex often precede tropospheric circulation anomalies by up to 2 months. The annular mode was found to dominate polar vortex fluctuations during the cold season. *Kodera et al.* [1990] showed that mesospheric wind disturbances progressed downward with time into the stratosphere in the National Meteorological Center/Climatic Analysis Center (NMC/CAC) data and in general circulation model (GCM) simulations up to 0.4 hPa, indicating mesosphere-stratosphere coupling. They showed that the signs of stratospheric sudden warmings (SSWs) began in the lower mesosphere and propagated downward to the troposphere. Recent observations have shown that mesospheric

cooling and MLT (mesosphere and lower thermosphere) zonal wind reversals occur prior to the stratospheric sudden warmings (SSWs) [e.g., *Hoffmann et al*., 2002; 2007; *Manney et al*., 2008a; 2009].

Interactions between the upper and lower atmospheres are complex and multifold, and coupling mechanism(s) are not well understood. Historically, observations have been limited to the altitudes below the stratopause (most below the middle stratosphere) because high-altitude data have not been available, and meteorological analyses become progressively more unreliable above the middle stratosphere [e.g., *Manney et al*, 2008a].

Here, we use Aura Microwave Limb Sounder (MLS) daily GPH data to, for the first time, derive the structure of the winter NAM and other leading EOF modes from the upper troposphere through the mesopause. These results are also used to study the mesosphere-stratosphere coupling during the major SSWs in 2006 and 2009 [e.g., *Manney et al*., 2008a; 2009] by focusing on the new results above the stratosphere.

2. Data and Methods

The data used in this study are the version 2.2 (v2.2) daily GPH from Aura MLS, which provides a GPH retrieval on 35 pressure levels from the upper troposphere (316 hPa) through the mesopause (~0.001 hPa; ~90km). Since the launch of NASA's Aura satellite in July 2004, the MLS instrument has been providing near-global daily observations in the middle atmosphere from mesosphere to the upper troposphere. The GPH measurement error generally increases with height, estimated to be 100 m or less for 10 hPa to 0.046 hPa, and 500 – 750 m at 0.001 hPa. MLS GPH accuracy and

precision are both ~100 m in the mid stratosphere and ~150 m at 316 hPa. Details on validation of the MLS geopotential height field are discussed by *Schwartz et al*. [2008].

We adopt the method in *Baldwin and Dunkerton* [1999; 2001] to calculate the NAM indexes. The MLS GPH field is mapped into 4 (latitude) x 8 (longitude) grid point from the average of daily ascending and descending orbits. A winter time (DJF) mean over the five years of MLS GPH observation period has been removed at each grid point at a given altitude to calculate the daily GPH anomalies. Daily MLS observations between 20°N and 84°N during the winter months (December to February) are used to derive the winter annular mode at each of MLS retrieval level. Data are weighted by the square root of cosine of latitude for equal area measurements at each grid point. The first winter mode is defined as the first EOF of the temporal covariance matrix of daily MLS GPH anomalies during DJF months in 2004-2009, and the EOFs are extracted independently at each pressure level.

3. Results and Discussions

3.1 Structures of the wintertime NAM

Figure 1 shows the first six EOF patterns for the winter NH at selected pressure levels. The first mode appears to be robust and significant at all MLS pressure levels. According to the criterion of *North et al.* [1982], the eigenvalues of the EOF modes have sampling uncertainties $\Delta \lambda_k \sim \lambda_k \sqrt{2/N}$ when the covariance matrix is constructed on the basis of N independent samples ($N \sim 433$). The spacing from first to second mode is greater than this sampling uncertainty in all MLS pressure levels. The pattern of the first mode at the surface, known as an Arctic Oscillation (AO), has higher amplitudes in the polar region and the well-known dipole structure in which the sub-

tropics have the opposite sign from the polar regions [*Thompson and Wallace*; 1998]. However, the patterns of the first EOF in the stratosphere and in the mesosphere have the same sign throughout the northern hemisphere, with amplitudes higher in the pole and decreasing towards the low latitudes. The second and third EOF modes have a higher variance over the persistent Aleutian High which is anti-correlated with the variability over the Icelandic Low. The second and third modes can be viewed as a pair of wave 1 patterns with the orthogonal orientation rotating slightly with altitude. Eigenvalues of these two modes are not well separated, suggesting that these modes are closely connected to each other. These two modes are ranked consistently at all altitudes in the second and third place in terms of variance contribution. *Lee and Hameed* [2007] discussed characteristics of the first and second modes in the troposphere and the stratosphere using monthly averaged NCEP/NCAR reanalysis, and *Lee et al*. [2008] compared the characteristics of these modes with the GISS (Goddard Institute of Space Science) GCM. The comparison of patterns derived from the 5-year MLS record and those from the 57-year NCEP/NCAR reanalysis (Figure 1) show consistent patterns, suggesting that the NAM signal is robust independent of the length of the record used in the analysis.

The relative importance of the leading EOF modes of MLS wintertime GPH variability is shown in Figure 2 in terms of percentage of variance contribution. The sum of the first six modes accounts for up to 95 percent of the total variance of the geopotential height field in the mesosphere. The first NAM pattern explains more than 65 % of the wintertime variance at all levels between 0.01 and 10 hPa. The dominance of NAM in the GPH variability of the middle atmosphere is a manifestation of the wintertime polar atmosphere is, to the first order, in the radiative equilibrium [*Shepherd*,

2007]. Propagating planetary and gravity waves that reach the mesosphere have amplitudes that grow with height, becoming the dominant dynamical forcing in the upper mesosphere. Since waves are associated with a broad spectrum of variability, the dominance of wave forcings reduces the percentage of variance captured by the first mode. In the high-latitude mesosphere, the amplitudes of gravity waves are at least as significant as those of quasi-stationary planetary waves, such as tides [e.g., *Offermann et al*., 2009]. Similarly, the upper tropospheric NAM minimum at ~300 hPa, with less than 20% of the total variance, is likely associated with large amplitudes of small-scale variability, such as gravity waves [e.g., *Namboothiri et al*., 2008].

The NAM of the MLS GPH variability at 316 hPa represents ~17 % of the total variance, but the observations are not available below 316 hPa [*Schwartz et al., 2008*]. The percentage of the AO (the pattern of the first mode near the surface), derived from the longer-term monthly NCEP data, is slightly higher than that of the mode in the upper troposphere from the daily MLS data from a relatively short period (~ 5 years): 21% from a 57-year analysis [*Lee and Hameed,* 2007], 23% from 40 years of five levels data [*Baldwin and Dunkerton*, 1999], and 22% from 97 years of sea level pressure data [*Thompson and Wallace*, 1998]. Because the first modes at 300-500 hPa account for ~4% less than those near the surface in the NCEP DJF analysis, the 17% of variance at 316 hPa from MLS is comparable to the variances estimated from long term analysis. In the stratosphere up to 10 hPa, the NAM accounts for substantially more (by about 20 %) variance in the MLS data than what was reported in *Lee and Hameed* [2007] from the NCEP/NCAR reanalysis. This is likely caused by greater variability from additional forcing factors, such as decadal variability, volcanic eruptions, and anthropogenic impact, which tend to reduce the contribution of the stratospheric NAM

from the long term analysis. The second and third modes are not well separated, always showing the orthogonal patterns to each other. Thus, the variances carried by these modes can be interpreted together. Together with the NAM mode, the first three leading modes of SLP AO from a 200-year simulation with the Canadian Centre for Climate Modelling and Analysis (CCCma) coupled climate model [*Fyfe et al*., 1999] account for similar variances (24%, 11%, and 9% of the total variance, respectively).

Figure 3 illustrates the different patterns of the NAM mode in extremely positive and negative phases. Variations between phases may occur within the same winter or from year to year. In the positive phase, MLS GPH in the mesosphere decreases poleward with a well-like shape centered on the pole, indicating a strong polar vortex in the winter middle atmosphere with strong descent inside the vortex. The low-index NAM pattern is characterized by a shallow, less-defined GPH well with a weak vortex, which may have multiple minimums at midlatitudes. Thus, the high-index NAM represents accentuation of the wintertime mean GPH distribution with low geopotential at the pole and strong meridional gradient. The low-index NAM represents a relatively flat GPH field with a weak meridional gradient.

3.2 The NAM signal in the middle atmosphere

Recent works have shown that there is large variability in winter middle atmosphere during the Aura MLS observation period [e.g., *Siskind et al*., 2007; *Manney et al*., 2008b; *Coy et al*., 2009]. *Rex et al.* [2006] suggested that extremely low stratospheric temperature in 2005 likely caused the largest amount of polar stratospheric clouds during the past 40 years. On the other hand, two unusually strong major SSWs occurred in 2006 and in 2009, followed by anomalous cooling in the upper stratosphere

[e.g., *Manney et al*., 2008a; 2009]. Major SSWs resulted in an abrupt increase in stratospheric temperatures in January 2006 and 2009, during which the polar vortex was distorted in a downward-progressive development, and shifted off the pole in 2006 but split in 2009.

The EOF analysis provides a powerful tool to extract and monitor the dominant patterns in the middle atmospheric dynamics. As seen in Figure 4, there is clear interannual variability in the wintertime stratospheric and mesospheric NAM. The positive NAM, corresponding to a strong polar vortex and low temperatures, is dominant in the lower mesosphere and the upper stratosphere in December 2004 and early January 2005. This positive phase continues to dominate the stratospheric variability until late February 2005, providing a favorable cold condition for forming PSCs in the lower stratosphere. In contrast, strong and persistent negative phases of the NAM are dominant in the mesosphere during January 2006 and 2009. Both winters are characterized by a weakened mesospheric polar vortex with significant easterly anomalies extending down to the upper stratosphere in January. The negative NAM phases in January 2006 and 2009, which were associated with easterly zonal wind anomalies in the stratosphere, signaled the major SSWs. The rapid changes of the mesospheric NAM to positive in February 2006 and 2009 capture the fast, strong reformation of the vortex after the warming [*Manney et al*., 2008a; 2009]. The positive NAM patterns are initiated in the mesosphere in late January and progress gradually into the upper stratosphere in February. The change from negative to positive NAM phases in the mesosphere precedes the upper stratospheric changes by ~4 weeks in the SSW years while the negative phases persist throughout February in the middle to lower stratosphere. The progression of the mesosphere-to-stratosphere

NAM captures the relatively slow recovery of the middle and lower stratospheric vortex.

In the stratosphere, the NAM index is a manifestation of the strength of the polar vortex, and its variability is thus largely driven by the wave forcing [*Haynes*, 2005]. In mid January of 2006 and early January of 2009, when a major stratospheric warming begins, a strong positive phase had also developed in the mesosphere in the second and third EOF modes (not shown). This positive phase indicates the strengthening of the wave 1 in response due to forcing from the troposphere [*Manney et al.*, 2008a; 2009]. Mid-latitude GPH maxima associated with an eastward-propagation ridge forcing which leads the poleward wave propagation triggered the stratospheric vortex breakdown in 2006 warming [*Coy et al*., 2009]. In contrast, strong negative phases in the decaying stage of the warming period in those Februaries indicate that the vortex is reforming in the mesosphere as the wave 1 response is no longer being forced from the troposphere.

4. Conclusions

The Aura MLS GPH data from mid-2004 to present provide new observations with which to characterize the spatial pattern and temporal evolution of the northern annular mode (NAM) in the entire middle atmosphere. We have analyzed the daily MLS GPH data to extract the first six EOF modes of the middle atmospheric variability and their interannual variations during the boreal winter.

During the winter season, the NAM is the most robust mode throughout all altitudes from the upper troposphere to the mesosphere, capturing up to 70% of the total wintertime variance. This is the first time that the NAM has been reported in the mesosphere, which completes the view of the NAM as the leading wintertime dynamic pattern. It has the strong presence throughout the mesosphere before decreasing near

the mesopause. The NAM dominance between 100 hPa and 0.01hPa is a manifestation of a radiatively-controlled polar middle atmosphere with the upper boundary near the mesopause. The lower boundary of the middle-atmospheric NAM, characterized by a minimum (17%) variance, is close to the tropopause.

The second and third EOF modes are a pair of orthogonal wave 1 patterns with orientation varying with altitude. The patterns derived from 5 years of daily MLS data are similar to those obtained from the longer-term analysis, suggesting that the modes are largely independent of the length of data record. Stratospheric sudden warmings (SSWs) are captured as large anomalies in the EOF modes. Anomaly patterns in the time-height development of the NAM index reveal downward progression from the middle mesosphere to stratosphere. Strong mesospheric cooling anomalies precede the major SSWs by up to ~4 weeks. The evolution of the vertically-distributed NAM indices clearly shows that SSWs begin with negative NAM perturbations in the mesosphere.

The EOF modes in the mesosphere and their interactions with the stratosphere require further investigations. The MLS observations support the view that the NAM structures in the stratosphere and mesosphere are controlled by a closely coupled system. The extensive MLS observations in the entire middle atmosphere provide a comprehensive view of dynamical links between the lower and upper atmospheres and their interactions during the SSW events. Large disturbances in the mesosphere often influence the entire stratosphere, and propagate further down to the surface via the stratosphere-troposphere coupling mechanism [*Holton et al., 1995*]. These dynamical processes can affect transport and chemistry of atmospheric constituents (e.g., ozone, H_2O, CO), of which the EOF analyses are under investigation.

Acknowledgments

We thank the MLS Science Team for their continuing support, especially Jung Hyo Chae, and Robert P. Thurstans for their programming and technical support. We also thank to Kirstin Krüger, Alexander Ruzmaikin, and Joan Feynman for inspiring discussions. This research was supported by an appointment to the NASA Postdoctoral Program at the Jet Propulsion Laboratory, administered by Oak Ridge Associated Universities through a contract with NASA. Research at the Jet Propulsion Laboratory, California Institute of Technology, is done under contract with the National Aeronautics and Space Administration.

"Copyright 2009 California Institute of Technology. Government sponsorship acknowledged."

References

Baldwin, M. P. and T. J. Dunkerton, (1999), Downward propagation of the Arctic oscillation from the stratosphere to the troposphere. *J. Geophys. Res*. *104* (D24), 30,937- 30,946.

Baldwin, M. P. and T. J. Dunkerton (2001), Stratospheric harbingers of anomalous weather regimes. *Science*, *294*, 581-584.

Baldwin, M. P. and T. J. Dunkerton (2004), The solar cycle and stratosphere-troposphere dynamical coupling. *Journal of Atmospheric and Solar-Terrestrial Physics*, **67**, 71-82.

Black, R. X. (2002) Stratospheric forcing of surface climate in the Arctic oscillation. *J. Clim.,* **15,** 268-277.

Coy, L., S. Eckermann, and K. Hoppel (2009), Planetary wave breaking and tropospheric forcing as seen in the stratospheric sudden warming of 2006, *J. Atmos. Sci.*, *66*, 495–507.

Fyfe, J. C., G. J. Boer, and G. M. Flato (1999), The arctic and Antarctic oscillations and their projected changes under global warming. *Geophys. Res. Lett*., **26**, 1601-1604.

Hameed, S., and J. N. Lee (2005), A mechanism for sun climate connection*, Geophys.*

Res. Lett., **32** (L23817), doi:10.1029/2005GL024393.

Hardiman, S. C., and P. H. Haynes (2008), Dynamical sensitivity of the stratospheric circulation and downward influence of upper level perturbations, *J. Geophys. Res*., **113**, D23103, doi:10.1029/2008JD010168.

Haynes, P. H. (2005), Stratosphere-Troposphere coupling, SPARC news letter, 25. http://www.atmosp.physics.utoronto.ca/SPARC/News25/index.html

Hoffmann, P., W. Singer and D. Keuer (2002), Variability of the mesospheric wind field at middle and Arctic latitudes in winter and its relation to stratospheric circulation disturbances, *J. Atmos. Solar-Terr. Phys.*, 64, 1229-1240.

Hoffmann, P.,W. Singer, D. Keuer, W. K. Hocking, M. Kunze and Y. Murayama (2007), Latitudinal and longitudinal variability of mesospheric winds and temperatures during stratospheric warming events, *J. Atmos. Solar-Terr. Phys.*, 69, 2355-2366, doi:10.1016/j.jastp.2007.06.010.

Holton, J. R., P. H. Haynes, M. E. McIntyre, A.R. Douglass, R. B. Rood, and L.Pfister, Stratosphere-troposphere exchange, *Rev. Geophys.*, *33*, 403–439,1 995..

Kodera, K., K. Yamazaki, M. Chiba, and K. Shibata (1990), Downward propagation of upper stratospheric mean zonal wind perturbation to the troposphere, *Geophys*

Res. Lett., **17,** 1263-1266.

Kushner, P. J. and L. M. Polvani (2004), Stratosphere–Troposphere coupling in a relatively simple AGCM: The role of Eddies. *J. of Climate*, **17**(3), 629-639.

Lee, J. N., and S. Hameed (2007), The Northern Hemisphere annular mode in summer: Its physical significance and its relation to solar activity variations, *J. Geophys. Res*., **112**, D15111, doi:10.1029/2007JD008394.

Lee, J. N., S. Hameed, and D. T. Shindell (2008), The northern annular mode in summer and its relation to solar activity variations in the GISS ModelE, *J. of Atmos. and Solar-Terr.Physics*, **70/5**, 730-741, doi:10.1016/j.jastp.2007.10.012.

Limpasuvan, V., and D. L. Hartmann (2000), Wave-maintained annular modes of climate variability. *J. Climate*, **13**, 4414-29.

Manney, G. L., K. Kruger, S. Pawson, K. Minschwaner, M. J. Schwartz, W. H. Daffer, N. J. Livesey, M. G. Mlynczak, E. E. Remsberg, J. M. Russell III, J. W. Waters (2008a), The evolution of the stratopause during the 2006 major warming: Satellite data and assimilated meteorological analyses, *J. Geophys. Res.*, **113**, D11115, doi:10.1029/2007JD009097.

Manney, G. L., W.H. Daffer, K.B. Strawbridge, K.A. Walker, C.D. Boone, P.F. Bernath, T. Kerzenmacher, M.J. Schwartz, K. Strong, R.J. Sica, K. Kruger, H.C.

Pumphrey, L. Froidevaux, A. Lambert, M.L. Santee, N.J. Livesey, E.E. Remsberg, M.G. Mlynczak, and J.R. Russell III (2008b), The High Arctic in Extreme Winters: Vortex, Temperature, and MLS and ACE-FTS Trace Gas Evolution, *Atmos. Chem. Phys*. **8**, 505-522.

Manney, G. L., M. J. Schwartz, K. Kruger, M. L. Santee, S. Pawson, J. N. Lee, W. H. Daffer, R. A. Fuller, N. J. Livesey (2009), Aura Microwave Limb Sounder Observations of Dynamics and Transport During the Record-breaking 2009 Stratospheric Major Warming, *Geophys. Res. Lett.*, in review.

Namboothiri, S. P., J. H. Jiang, P. Kishore, K. Igarashi, C. O. Ao, and L. J. Ro mans (2008), CHAMP observations of global gravity wave fields in the tr oposphere and stratosphere, J. Geophys. Res., 113, D07102, doi:10.1029/20 07JD008912.

North G. R., T. L. Bell, R. F. Cahalan, and F. J. Moeng (1982), Sampling errors in the estimation of empirical orthogonal functions. *Mon. Wea. Rev*., **110**, 699-706.

Offermann, D., Gusev, O.; Donner, M., Forbes, J. M.; Hagan, M., Mlynczak, M. G., Oberheide, J., Preusse, P., Schmidt, H., Russell, J. M., III (2009), Relative intensities of middle atmosphere waves, *J. Geophys. Res*., **114**, D6, D06110 doi:10.1029/2008JD010662

Plumb, R. A., and K. Semeniuk (2003), Downward migration of extratropical zonal wind anomalies, *J. Geophys. Res.*, 108(D7), 4223, doi:10.1029/2002JD002773.

Rex, M., Salawitch, R. J., Deckelmann, H., von der Gathen, P., Harris, N. R. P., Chipperfield, M. P., Naujokat, B., Reimer, E., Allaart, M., Andersen, S. B., Bevilacqua, R., Braathen, G. O., Claude, H., Davies, J., Backer, H. D., Dier, H., Dorokhov, V., Fast, H., Gerding, M., Godin-Beekmann, S., Hoppel, K., Johnson, B., Kyrö, E., Litynska, Z., Moore, D., Nakane, H., Parrondo, M. C., Jr., A. D. R., Skrivankova, P., Stubi, R., Viatte, P., Yushkov, V., and Zerefos, C.: Arctic winter 2005: Implications for stratospheric ozone loss and climate change (2006), *Geophys. Res. Lett*., 33, L23808, doi:10.1029/2006GL026731.

Shepherd, T. G. (2007), Transport in the middle atmosphere, *J. Meteorol. Soc. Japan*, **85B**, 165– 191.

Schwartz, M. J., et al. (2008), Validation of the Aura Microwave Limb Sounder temperature and geopotential height measurements, *J. Geophys. Res.*, 113, D15S11, doi:10.1029/2007JD008783.

Siskind, D. E., , S.D. Eckermann, L. Coy, and J. P.McCormack (2007), On recent interannual variability of the Arctic winter mesosphere: Implications for tracer descent, *Geophys. Res. Lett.*, *34*, L09806, doi:10.1029/2007GL029293.

Thompson D. W. J. and J. M. Wallace (1998), The Arctic Oscillation signature in the wintertime geopotential height and temperature fields. *Geophys. Res. Lett.,* **25***,* 1297-1300.

Thompson D. W. J., and J. M. Wallace (2000), Annular modes in the extratropical circulation. Part I: Month-to-month variability. *J. Clim.,* **13**, 1000-1016.

Figures

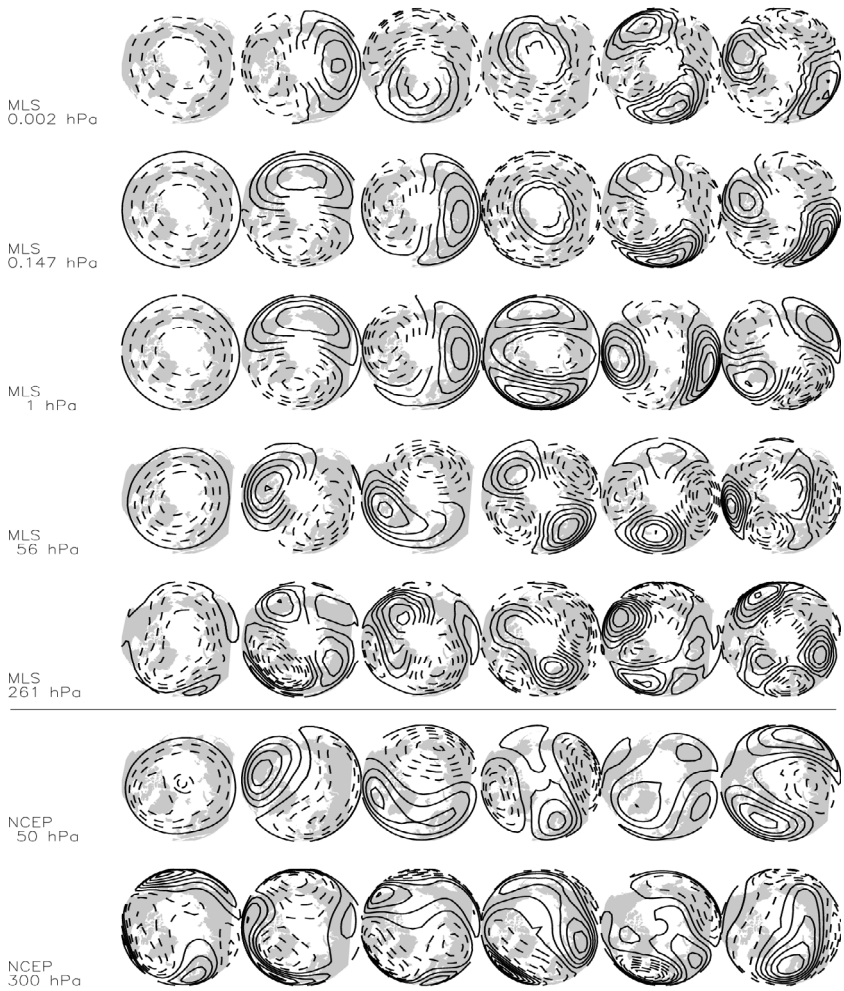

Figure 1. NAM patterns for winter (from December to February) at 0.002 hPa, 0.147 hPa, 1 hPa, 56 hPa, and 261 hPa. The solid contours represent the positive values from zero, and dashed contours are negative values. Contour interval is 0.02. The patterns from MLS are calculated as the first six EOFs of MLS daily geopotential height for 2004-2009. NAM patterns for winter (from December to February) with NCEP/NCAR reanalysis are also shown at 50 hPa and 300 hPa. The patterns from the reanalysis are calculated as the first six EOFs of monthly geopotential height for 1948-2008.

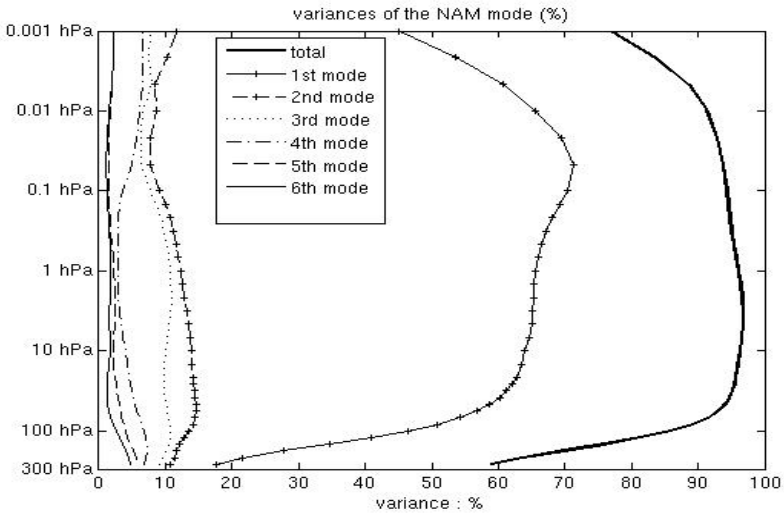

Figure 2. Variance of the each modes of NAM patterns (left) and integrated variance of the first seven modes (right). The patterns are calculated as the first and higher EOFs of daily geopotential height for 2004-2009.

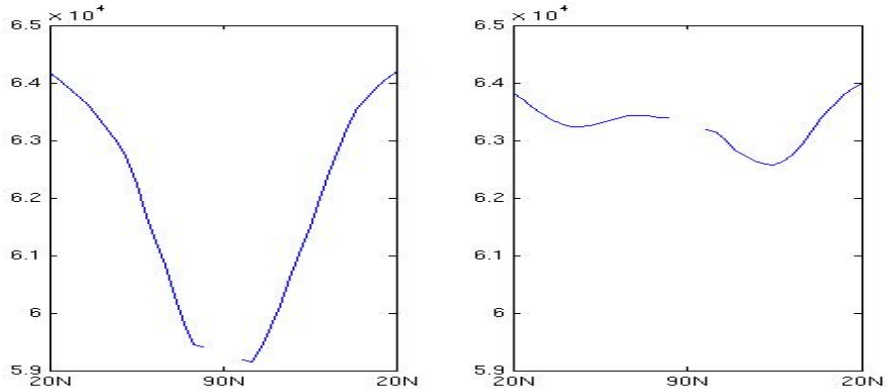

Figure 3. The cross sections of the MLS GPH across 90W to 90E for high (pc >17) NAM index (left) and low (pc<-17) NAM index (right) at 0.1 hPa in the winter period (December-February). To derive these composite patterns, 69 days above one standard deviation of the NAM index and 55 days below one standard deviation of the index are averaged, respectively.

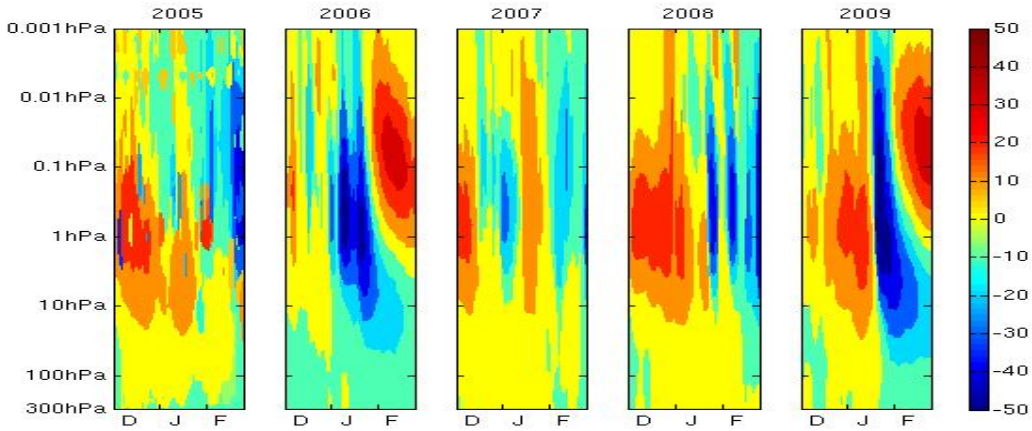

Figure 4 Time-height development of the first mode during winters of 2005-2009. Red represents positive index (a cold condition with the strong polar vortex).